

# SOILS BACKGROUND INVESTIGATIONS AT THE JEFFERSON PROVING GROUND UXO TEST SITES: IMPLICATIONS FOR DETECTION AND DISCRIMINATION

Dwain K. Butler and José L. Llopis  
U.S. Army Engineer Research and Development Center  
3909 Halls Ferry Road, Vicksburg, MS 39180-6199  
Telephone: 601-634-2127; FAX: 601-634-3453  
E-Mail: *butlerd@mail.wes.army.mil*

Category: Detection Technology Session

## Abstract

The four demonstration phases at Jefferson Proving Ground (JPG) document some significant advances in unexploded ordnance (UXO) detection, discrimination, and identification capability. The JPG sites, originally thought to be simple sites for the UXO technology demonstrations in terms of geologic and cultural clutter backgrounds, have characteristics that make UXO detection difficult, even problematic. Detection of UXO must be accomplished in the presence of these backgrounds. There are inherent limitations on the detection capability of geophysical systems caused by the size and depth of burial of UXO (a given UXO may be too small and/or too deep to produce a detectable anomaly signature), and these limitations exist regardless of the geologic and clutter backgrounds. The geologic background further decreases UXO detectability by attenuating signatures, reducing physical property contrasts, and providing sources of localized anomalies. The cultural background or clutter decreases the reliability of UXO detection due to interference signals and false alarm anomalies caused by surface and buried cultural features.

Geophysical properties vary spatially and temporally at the JPG sites. Electrical and electromagnetic property variations as function of position, depth, and time are analyzed. Demonstrators have noted anomalous magnetic signatures at the site that have been attributed to soil variations. These magnetic anomalies are investigated by acquiring in situ magnetic susceptibility measurements. A simple magnetic susceptibility model along a profile line is constructed from the measurements, and a total field magnetic anomaly is computed that is in qualitative agreement with the observations. The large observed and computed magnetic signatures illustrate how magnetic susceptibility variations in the shallow subsurface can complicate UXO detection. Soil types and properties and spatial and temporal variations in electrical conductivity and dielectric permittivity explain the past difficulty in detection of UXO with ground penetrating radar systems at the site. Conductivity and magnetic susceptibility variations also pose problems for electromagnetic induction systems at the sites.

## Background

The JPG Phase IV UXO Technology Demonstrations included a science and technology (S&T) program, directed to answering outstanding questions and perceived deficiencies of the JPG program (Butler et al 1998). The S&T program included supplemental site characterization, establishment of a standardized 1-hectare site, assessments of prior JPG Phases, Phase III demonstrator self-assessments, monitoring Phase IV demonstrations, geophysical signature modeling for baseline targets, and phenomenological studies of spatial and temporal variation of environmental and geophysical parameters and associated effects on UXO detectability. This paper surveys the phenomenological studies; complete results are found in Butler et al (1999).

## Introduction to the Phenomenological Studies

In UXO detection and discrimination surveys, the geophysical sensor responses are a superposition of the signatures of (a) the host medium, (b) cultural sources and (c) the buried ordnance. Signatures due to the host medium and cultural sources constitute the background. Part of the response to the host medium will be due to materials (soil and rock) below the depth of burial of the UXO as well as surface topography. The host medium will generally be heterogeneous both vertically and horizontally on multiple size-scales (e.g., Butler 1975, Isaaks and Srivastava 1989, Sahimi 1995). Sometimes the host medium may contain rocks or tree roots or animal burrows comparable in size to the buried ordnance. In some cases the geophysical methods used for detection and discrimination of buried UXO may be relatively unaffected by the nature of the host medium, such as magnetic surveying for UXO buried in many typical soils. However, there are conditions where the nature of the host medium makes buried UXO detection problematic (e.g., Khadr et al. 1997), such as:

- (a) high electrical conductivity soils that produce large electromagnetic (EM) induction responses and attenuate ground penetrating radar (GPR) signals after short distances of propagation;
- (b) soils with high magnetic susceptibility or included rocks with high magnetic susceptibility;
- (c) large rocks, tree roots, and animal burrows that produce GPR signatures similar to UXO;
- (d) mixed, highly heterogeneous soils, with short spatial wavelength variability in electrical conductivity, dielectric permittivity, and/or magnetic susceptibility.

Cultural sources that contribute to sensor responses are: (1) objects (“clutter”) on the surface or buried in the host medium, such as exploded ordnance debris and other metallic objects; (2) interference from EM transmitters/emitters of various types. The geophysical signatures of buried ordnance depend on (a) size, shape, depth, orientation, composition, and physical properties of the ordnance, (b) physical properties of the host medium, and (c) inclination and declination of the local earth’s magnetic field. Whether or not the geophysical signatures of buried ordnance are detectable depends on the magnitudes, spatial wavelengths, and other features of the signatures relative to the signatures of all other sources, i.e., the background. However, signatures of buried ordnance, that might be “theoretically” detectable in a given setting, may not be detected in practice due to the details of the data acquisition process, e.g., inadequate sampling or measurement spacing.

### **Significant Environmental and Climatic Factors**

The climate of JPG is described as moist, moderately humid, and cold in the winter and hot in the summer (Nickell 1985; McWilliams 1985). The primary environmental and climatic factors that can affect geophysical sensor response, are wind speed, vegetation, temperature, and rainfall. These data and other environmental parameters were acquired during the Phase IV demonstrations. The temporal variability of these factors are important for assessing or comparing performance of different geophysical systems and demonstrations at different times.

**Wind speed.** Wind speed and changes in speed and direction primarily affect gravity and seismic measurements, directly through flow against and around the sensor cases and indirectly through ground-coupling. Wind speed and direction at JPG are highly variable, but generally will not pose an instrument vibration problem except during thunderstorms and other severe weather. The prevailing winds are from the south, and the *average* wind speed is *highest* in the spring, about 5 m/s (11 mph). Gravity and seismic methods have not been used to date for UXO technology demonstrations at JPG.

**Vegetation.** Vegetation affects measurements with all of the geophysical methods. Larger trees and shrubs alter the uniformity of measurement grids and result in areas of no measurements. Variation in height of grasses will result in increased noise levels due to causing sensor elevation and orientation variations during surveys. Trees and tree roots can produce EM induction and GPR sensor responses that may be misinterpreted as anomalies caused by buried UXO (false alarms). Also, tree canopies can prevent the use of GPS for site navigation. The grass cover on the 40-acre site was kept mowed to a height of 10-20 cm during the demonstrations, particularly for Phases II to IV. Other vegetation on the 40-acre site is scattered and generally isolated, ranging from shrubs to mature trees. Generally the trees will interfere with measurements for a radius of 1 to 2 m. There are a few areas on the site where closely spaced trees or large trees with low growing limbs can interfere with measurements over an area with radius up to 5 m.

**Temperature.** Air and subsurface temperatures affects sensor response in three ways: (1) instrumental noise and drift for some sensors is sensitive to ambient temperatures; (2) changes in dimensions of components in a system can result in altered measurement geometry; (3) subsurface physical properties can vary with temperature. Subsurface physical property variation with temperature is generally small for temperatures above the freezing point, e.g., a 10 deg C temperature change will result in approximately a 20 per cent change in electrical resistivity for electrolytic conduction in water saturated soil and rock. For relatively dry soil and rock, the change in electrical resistivity with temperature is quite small. For temperatures below the freezing point, the electrical resistivity is 1 to 2 orders of magnitude larger than at temperatures above the freezing point (Keller and Frischknecht 1970). The affects of temperature on instrument noise, drift, and altered measurement geometry are completely sensor system dependent and require assessment for each system.

At JPG the average daily temperature range in winter is approximately -4 to 7 deg C (25 to 45 deg F), and in summer is approximately 18 to 30 deg C (65 to 87 deg F). Thus there is an average 10 to 12 deg C temperature change in any 24-hour period of the year and the temperature effect on resistivity for saturated soil conditions at JPG will typically be 20 percent or less in any 24-hour period. The effect of temperature change on resistivity between the

extreme temperatures in summer and winter could be significant for saturated materials. However, the depth to “permanently saturated” materials in the area of the 40-acre site exceeds the subsurface depth extent of the annual and diurnal temperature changes. Significant periods of temperatures below freezing are not common, and the depth of freezing in soil is limited to a few centimeters.

### **Topography, Site Conditions, and Soil Series Maps**

The topography of the JPG sites is gently rolling with minor drainage paths crossing the sites (Llopis et al 1998; Nickell 1985; McWilliams 1985). Cultural reshaping of the natural topography is minor, consisting of tire tracks, foot paths, small excavated soil mounds, and depressions resulting from ordnance burial activity associated with the demonstrations. After heavy rainfall, the tire tracks and other depressions fill with water, due to low permeability near-surface soils and are thus readily apparent. For the Phase I demonstrations, the sites were tilled prior to the technology demonstrations to conceal the ordnance burial sites, leaving a highly irregular small scale surface topography; the sites were not tilled for the subsequent phases.

For the 40-acre site, the maximum topographic variation is 8.8 m, with a well-developed drainage path from east to west and northwest across the northern part of the site (Figure 1). Topography and site conditions affect geophysical surveys in three ways, that are not necessarily interrelated: (1) rugged topography inhibits coverage with vehicular mounted sensor systems; (2) small scale topography introduces noise and “false alarm” anomalies; (3) topography correlates with soil type, soil moisture conditions, other soil properties which affect measurements, and vegetation. There are only minor vehicular access problems due directly to topography at the JPG sites; however, indirectly topography restricts vehicular system access to some areas of greater than normal density vegetation. The site tilling done for Phase I caused considerable survey problems for vehicular-mounted demonstration systems and created a major source of false alarms for the GPR systems. The noise levels for all survey systems in Phase I, both hand-held and vehicular-mounted, was increased due to varying sensor height and orientation relative to the surface and the buried ordnance.

Soil unit definitions and descriptions include typical surface slopes, thus it is not surprising that there should be some correlation between soil types and topography (Nickell 1985; McWilliams 1985). An overlay of topography and the general soils map for the 40-acre site (Llopis et al 1998) is given in Figure 2. Other correlations between topography and soil types and geophysical properties are noted in the following sections.

### **Soil Water Content**

Soil water content is the major time-dependent subsurface variable that affects geophysical sensor response. Above the water table, soil water content is time-variable due to rainfall, infiltration, and evapotranspiration. Below the water table, soil and rock are completely saturated and have time-independent water content. The rate of infiltration is controlled by the vertical hydraulic conductivity of the soils. JPG soils have very low hydraulic conductivity, typically 10-7 cm/s, leading to ponding conditions in depressions after rainfall, including tire tracks and settlement depressions over ordnance burial locations (PRC Environmental Management, Inc. 1994; Nickell 1985; McWilliams 1985).

During prolonged dry periods, the ground surface becomes very hard, and during prolonged wet periods, the ground surface becomes very soft. During prolonged wet periods, the significantly increased soil water content zone will extend to depths of 0.5 m or more, but after moderate rainfalls the “nearly saturated” zone is confined to the upper few centimeters. An example of soil water content variation with depth is shown in Figure 3, for soil samples collected on 3 August 1997 (very dry conditions) and 29 April 1998 (very wet conditions) at grid location G7, approximately in the center of the 40-acre site. The numbers in parentheses by the nine sampling locations (triangles) in Figure 1 are weight-based water contents from August 1997 at 10-, 50-, and 100-cm sampling depths; mean water content for 10-cm depth for the nine locations is  $13 \pm 1$  percent. For samples acquired at five locations in April 1998 at 10-cm depth, the mean water content is  $33 \pm 3$  percent.

For JPG Phase IV, water contents were determined for 10-cm and 50-cm samples from three locations on the 40-acre site (K1, G7, C13; see Figure 1) each week during the extent of the demonstrations. These water content data are shown in Figure 4 as a function of time. The August 1997 conditions are comparable to the driest conditions encountered during the Phase IV demonstrations (15 September 1998). The April 1998 water contents for location G7, however, are higher than values observed for any of the three locations monitored during the Phase IV

demonstrations. Thus the August 1997 and April 1998 site conditions effectively represent the extremes in shallow soil moisture during the period of investigations.

### Soils Classifications

Failure of surface and airborne GPR systems at JPG is attributed to high ground electrical conductivity (leading to high GPR signal attenuation), scattering, false alarms associated with rocks in the soil, and rough surface conditions (Altshuler et al 1995; USAEC 1995, 1996, 1997). The high ground conductivity and signal attenuation are commonly and logically attributed to high clay content soils, exacerbated by high water contents at certain times (USAEC 1996). The fact that the water content of the shallow soils (samples from  $\leq 1.0$ -m depth) varies considerably during the year is documented in the previous section. Shallow JPG soils, collected at 21 locations, classify as sandy clay, silty clay, and clay, based on particle size distribution, and as low to high plasticity clays, based on visual inspection (Llopis 1998; PRC Environmental Management, Inc. 1994). Engineering classification of the shallow JPG soils results in classification primarily as low plasticity clays. However, when plotted on a graph of engineering index parameters (Means and Parcher 1963; Cassagrande 1948), the JPG soils plot in a region of the space where soils can be either low plasticity clays or slightly plastic silts or very fine silty sands (see Figure 5; Llopis et al 1998). X-ray diffraction analyses of eight JPG soil samples reveal only trace amounts of clay minerals, with quartz being the predominant mineral (Llopis et al 1998). Thus the shallow JPG soils are very fine-grained, quartz silts and sands, and attenuation of GPR signals cannot be attributed to high clay content soils in the shallow subsurface. Results of field and laboratory investigations of past failures of GPR at the JPG sites are documented in Llopis et al (1998) and Arcone et al (1998).

### Variability of Geophysical Properties

**Geophysical site characterization.** The site characterization surveys investigated the horizontal and vertical variability of the geophysical parameters that affect sensor performance—the electromagnetic properties as a function of frequency and water content. Electromagnetic properties were determined by electrical resistivity sounding, terrain electromagnetic conductivity, in situ complex dielectric permittivity measurements, GPR surveys, and laboratory testing. From in situ and laboratory permittivity measurements, conductivity, loss tangent, attenuation factor, and phase velocity are determined as functions of frequency and water content.

The magnetic susceptibility of the natural geologic materials was not expected to vary significantly over the sites. Thus the original site characterization did not include investigations addressing the spatial or temporal variability of the magnetic susceptibility. However, feedback from Phase II and III demonstrators indicates some significant areas of magnetic anomalies that are presumed to be caused by mineralogic variations in the soils. Field magnetic susceptibility measurements were subsequently made over two of the most significant geologic anomaly areas.

### Electrical resistivity: Spatial and temporal variability considerations

**Conductivity Maps.** Electrical conductivity maps for the 40-acre site for dry (August 1997) and wet (April 1998) site conditions are shown in Figure 6. The maps indicate variability of soil and rock type and/or water content over the site. The EM system is a bistatic, frequency domain EM system that operates at 9.8 kHz. Depth of investigation of the system is nominally 4 to 5 m but is most strongly influenced by material in the upper 1 to 2 m. Each of the maps in Figure 6 illustrate the spatial variability of electrical conductivity for a given date, while comparing the two maps indicates the effects of different soil water content or intervening site disturbance on the conductivity distribution. As documented previously, the site conditions for the dates of the two maps in Figure 6 represent the “driest (left map) and the “wettest” site conditions (right map) for the period August 1997 to November 1998 at the JPG 40-acre site. There is a general correlation between the conductivity distribution and soil types (see Figure 6). The correlations between soil type and conductivity are complicated by the facts that (a) soil type correlates with topography and (b) generally the topography correlates with soil water content (higher elevation areas are typically dryer than lower elevation areas).

The general patterns of conductivity are similar in the two maps. Differences between the two maps relate to localized differences in soil water content or site disturbance, resulting from ponding of water in depressions and target burial activities between the times of the two maps. Simple statistical analyses of the values in the two conductivity maps are shown in Table 1. The *average (mean) and the standard deviation of the conductivity* increases only slightly (approximately 1 mS/m) from the dry to wet conditions map, although the *range of conductivity* values increases by a factor of 4 from the dry to wet conditions map.

<b>Statistic</b>	<b>Dry (Aug. 1997)</b>	<b>Wet (Apr. 1998)</b>
Minimum, mS/m	10.5	12.2
Maximum, mS/m	32.5	94.9
Average, mS/m	19.9	20.8
Standard Deviation, mS/m	3.6	4.8

**Electrical resistivity monitoring.** Vertical electrical resistivity soundings (VES) conducted on the 40- and 80-acre sites and the 1-hectare sites assess the vertical electrical resistivity variation. Detailed VES results and correlations with site geology are discussed by Llopis et al (1998). Generally the VES results indicate a 3- or 4-layer geoelectrical structure. For the 4-layer structure, simplified correlations with geology are: layer 1 — near surface, silty soils with high organic content and porosity; layer 2 – moist, silty materials; layer 3 – wet, higher clay-content materials; layer 4 – limestone. VES interpretations for grid location G7 for three dates are shown in Figure 7. The first two VES results (for August 1977 and October 1977) are for dry site conditions, while the third is for wet site conditions (April 1998). The major change from dry to wet site conditions is the dramatic decrease in layer 1 resistivity, from approximately 800 to 300 ohm-m.

Grid location G7, approximately at the center of the 40-acre, site served as a monitoring location for the Phase IV demonstrations. The major changes in the geoelectrical structure are in the resistivities and thicknesses of layers 1 and 2. The parameters for the upper two layers are well defined (resolved) in the inversions, while the resistivity and thickness of layer 3 are not well resolved (equivalence). A summary of the variation of the parameters of the interpreted geoelectrical sections for 7 VES is indicated in Table 2.

<b>Layer Parameter</b>	<b>Range</b>	<b>Mean</b>
Layer 1 — Resistivity, ohm-m	450–880	655
Layer 1 — Thickness, m	0.3–0.6	0.5
Layer 2 — Resistivity, ohm-m	80–160	135
Layer 2 — Thickness, m	1.0–1.6	1.2
Layer 3 — Resistivity, ohm-m	25–38	30
Layer 3 — Thickness, m	2.6–3.5	3.1

### **Dielectric Permittivity: Spatial and Water Content Variability**

The field and laboratory investigations of dielectric permittivity are thoroughly documented in Llopis et al (1998), for the frequency range 45 MHz to 4.045 GHz. Laboratory dielectric permittivity results are illustrated in Figure 8 for 200 MHz. Data plots for other frequencies are qualitatively similar. The plots in Figure 8, for all locations and all depths (surface to 1-m depth) on the 40- and 80-acre sites, are for the real and imaginary components of the relative complex dielectric permittivity and for the EM attenuation (dB/m) and conductivity (mho/m = 1000 mS/m) as a function of volumetric moisture content (percent). There is no obvious separation of values for samples from the 40- and 80-acre sites. For the 40-acre site, the real and imaginary components of the relative dielectric permittivity vary approximately linearly with volumetric moisture content between 10 and 40 percent, with a variation of less than  $\pm 2$  at any specific moisture content.

In addition to the laboratory dielectric permittivity measurements, two other field tests give insight to the spatial and frequency variation of the dielectric permittivity. Results of GPR surveys can be interpreted to give the *real part* of the complex relative dielectric permittivity, by conducting wide-angle reflection-refraction surveys and by analyses of diffraction hyperbolas. Llopis et al (1998) and Arcone et al (1998) present results of analyses of 70 hyperbolas in 300 MHz GPR profiles and 48 hyperbolas in 600 MHz GPR field profiles from the 40-acre site. Analyses of the results indicates no statistically significant difference in the mean and standard deviation of the real, relative dielectric

permittivity values for the 300 and 600 MHz data ( $10.5 \pm 4.2$  versus  $10.4 \pm 3.5$ , respectively). Dielectric permittivity determined from GPR survey data are representative of volume-average values over the propagation paths that define the hyperbolic events. An in situ probe was also utilized to investigate spatial dielectric permittivity variability (Llopis et al 1998). The DICON probe (Miller, Malone and Blount 1992) makes a point (small volume) measurement of the complex dielectric permittivity at 60 MHz. Measurements were made at 10- and 50-cm depths at 25 locations on the 40-acre site (Figure 9). The permittivity values increase with depth everywhere.

Table 3 summarizes the measurements or determinations of real, relative dielectric permittivity. The laboratory measurements are for a moisture content of 25 percent, an appropriate moisture content for the time of the GPR surveys and DICON probe measurements. The values of relative dielectric permittivity are consistent, and there is a general trend of decreasing relative dielectric permittivity as frequency increases.

<b>Test Type</b>	<b>Frequency, MHz</b>	<b>Relative Permittivity</b>
Laboratory	100	13
	200	11
	495	11
	1,015	10
GPR	300	10.5
	600	10.4
DICON Probe	60	19.2

### **Magnetic Susceptibility: Spatial Variability**

Magnetic susceptibility of near surface materials is not normally expected to vary significantly over short distances, particularly in a non-igneous terrain. It is not uncommon, however, for soils to have higher magnetic susceptibilities than the parent rocks due to selective sorting of heavy minerals (Burger 1992). Soil magnetic susceptibility can vary by factors of 2 to 3 over distances of tens of meters. Typical sedimentary rock susceptibilities average  $5 \times 10^{-4}$  (SI), while soil susceptibilities can be as high as 1 to  $1.5 \times 10^{-3}$  (SI). Commonly, the susceptibility variation of soils in an area (as portrayed in a histogram of values) will be unimodal with a rather narrow peak (Scollar et al 1990). Anomalously high or complex spatial variability of magnetic susceptibility were never suspected for the JPG sites.

During preparation for the JPG Phase IV demonstrations, the presence of significant, nonordnance-related anomalies of the magnetic field was revealed by some of the Phase II and III demonstrators. In addition to magnetic anomalies due to buried targets (ordnance and non-ordnance targets), the magnetic maps include other anomalies that can be attributed to cultural features and soil properties. An obvious cultural feature anomaly is the linear anomaly pattern that trends nearly due north-south along the western side of the 40-acre site that is caused by a fence. Another linear anomaly occurs between east-west grid lines 10 and 11 and is likely caused by the buried remnants of a fence. The longer spatial wavelength anomalies, many of which are subtle in expression, are presumably geologic in origin and likely from shallow sources. Two significant anomalous areas, that are not subtle, exist in the northeast and northwest quadrants of the site. These apparently anomalies follow the trends of drainage features across the 40-acre site.

Grid lines K and M and grid lines 4 and 6 approximately bound the large magnitude geologic anomaly feature in the northwest quadrant. More subtle expressions of the anomaly extend outside this area to the northeast and southwest, following the trends of drainage features. The magnetic anomaly map of this feature is shown in Figure 10, from the Naval Research Laboratory MTADS survey of the site during JPG Phase III (McDonald and Nelson 1999). Although the overall anomalous feature is complex, the most obvious aspect of the anomaly is a dipolar pattern, with a large magnitude negative band ( $\sim -130$  nT) to the south and a large magnitude positive band ( $\sim +115$  nT) to the north.

The obvious approaches to investigation of the causes of geologic-origin magnetic anomalies are to measure laboratory and in situ values of magnetic susceptibility and to conduct laboratory mineralogical analyses of soil and rock samples. Two types of measurements were obtained in situ in the anomalous areas. A frequency domain EM system (Geonics EM38) was used to acquire terrain conductivity and magnetic susceptibility measurements (McNeill 1986) over the area bounded by grid lines K, M, 4, and 6 (61- x 61-m or 200- x 200-ft area.). Measurements were acquired approximately on a 6- x 2-m grid for terrain conductivity and on a 6- x 6-m grid for magnetic susceptibility. Magnetic susceptibility measurements with the EM38 are estimated to be a volume-averaged values for the upper 0.5 m of the subsurface, relative to the magnetic susceptibility of air. Magnetic susceptibility measurements were also acquired with a laboratory magnetic susceptibility system (MS2) fitted with a field measurement search coil (Bartington MS2 Magnetic Susceptibility System; Bartington Instruments Ltd. 1994) on a 6-m grid within the same area as the EM38 measurements, and additionally MS2 measurements were acquired along grid lines K and L at approximately 30-m intervals (100 ft). MS2 magnetic susceptibility measurements are volume-averaged values for the upper 15- to 20-cm of the subsurface, relative to the magnetic susceptibility of air (Dearing 1994). For the MS2 measurements, surface vegetation was scraped away and the search coil placed in intimate contact with the soil. Both the EM38 and the MS2 magnetic susceptibility measurements are real-component, volume magnetic susceptibilities in SI units.

Results of measurements to investigate the nature of the northwest quadrant geologic magnetic anomaly are presented in Figures 11 to 13. The EM38 operates at 14.6 kHz and has a nominal depth of investigation of 1.5 m (vertical dipole mode) for conductivity measurements (McNeill 1986). The conductivity values are low throughout the area (1 to ~ 17 mS/m), with the northern half of the area having an anomalously low average conductivity of ~ 2 to 3 mS/m. The same relative patterns of conductivity are evident in Figure 6, where the conductivities are for a nominal 5-m depth of investigation.

The EM38 magnetic susceptibility map is shown in Figure 12. Significant variations (an order of magnitude) in magnetic susceptibility occur over horizontal distances of 10 m or less. There are no obvious correlations to terrain conductivity (Figures 6 and 11). However, the correlation to the northwest quadrant total magnetic field anomaly (Figure 10) is evident. Figure 13 shows the MS2 magnetic susceptibility measurements along line K; compared to the EM38 values where they overlap. The magnetic susceptibility along lines K and L both show a systematic decrease in values from approximately  $6 \times 10^{-4}$  (SI) in the north to approximately  $1 \times 10^{-4}$  (SI) in the south, with anomalous values in the area of the northwest quadrant magnetic anomaly. The EM38 and the MS2 values show the same trends in the anomalous area. Proceeding from south to north, a high-low-high pattern is noted. The EM38 values are higher in magnitude, indicating that magnetic susceptibility increases with depth in the anomalous area (at least in the upper 0.5 m of the subsurface).

### **Observations and Implications**

The dominant environmental variable, affecting geophysical parameters and subsurface detection capability, is rainfall. Rainfall directly affects the soil water (moisture) content, which in turn plays a major role in determining the electrical resistivity (conductivity) and dielectric permittivity of subsurface materials. Due to the low hydraulic conductivity of near surface soils at JPG, rainfall tends to pond on the surface and infiltrate very slowly. Thus after small rainfall amounts, evaporation will dominate infiltration, particularly during the summer, and increased soil water contents will be limited to very shallow depths for short periods. Following large rainfall amounts, soil water contents are elevated to greater depths (0.5 m) and persist for longer periods (short and long periods are used as purely qualitative terms, since the present work did not quantify the effects). The average surface (~ 10 cm) natural soil water content during very dry site conditions is 13 percent (approximate range 11 to 15 percent), while the average surface water content during very wet site conditions is 33 percent (approximate range 28 to 38 percent). At a given location during dry site conditions, the water content will increase with depth (at least to 1-m depth); while during wet site conditions, the water content will decrease with depth. The water content measurements during Phase IV demonstrations indicate large fluctuations in surface water contents (as large as 20 percent), while the deeper (~ 50 cm) water content fluctuations are much smaller (5 to 7 percent).

The daily precipitation during the JPG Phase IV demonstrations is shown again in Figure 14, along with air and soil temperatures and the variation in parameters for the VES results. There are no obvious correlations between the VES parameters and temperature. There is a significant rainfall event (1.2 in. or 3 cm) on 20 September 1998, following a month with only trace amounts of rainfall. Following the rainfall event, the layer 1 thickness increases by

approximately 0.4 m (with a corresponding decrease in layer 2 thickness) and the resistivity decreases from 620 ohm-m to 500 ohm-m. The resistivity of layer 1 increases from 450 to 750 ohm-m, with some fluctuation, over the course of the Phase IV demonstrations as a result of increasingly dry conditions. The resistivity of layers 2 and 3 remain practically constant during the demonstrations.

Due to the depth of investigation (nominally 4 to 5 m) of the terrain conductivity maps in Figure 6, the affect of the shallow soil water content changes on conductivity are small. The major factor affecting the terrain conductivity is likely the clay layer present nearly everywhere beneath the 40- and 80-acre sites. Based on 25 VES results, the clay layer beneath the 40-acre site varies from approximately 1.5- to 5-m in thickness, and the depth to top of the clay layer varies from approximately 0.3 m to 2 m (Llopis et al 1998). For example shallow depth to top of clay (determined from the VES results) is the cause of the high conductivity features centered approximately about locations D3 and K7, while depth to clay is apparently not the cause of the high conductivity area that extends from approximately I13 to A7.

The conductivity and dielectric permittivity variations for shallow depths (< 1.0 m) indicate significant changes as a function of water content. The laboratory properties at 200 MHz shown in Figure 8 show significant changes as a function of water content; this is illustrated in Table 4 for the measured water content extremes for dry- and wet-site conditions. The parameter ranges in Table 4 reflect the scatter in measurement data over the site (see Figure 8) at or near the indicated water contents.

<b>Average Water Content, %</b>	<b>Real Component, Relative Dielectric Permittivity</b>	<b>Attenuation, dB/m</b>	<b>Conductivity, mS/m</b>
Dry Site Conditions — 13	4–6	4–8	6–10
Wet Site Conditions — 33	17–19	15–25	40–60

The negative implications of the spatial and temporal variations of geophysical parameters over the 40-acre site for buried object detection are primarily for the magnetic methods and GPR. While the variations in electrical conductivity (resistivity) do have some implications for the EM induction methods, the impact on detectability considerations is minor for the type methods normally employed for UXO detection. For the time domain EM (TDEM) methods that are typically used, the measurement time gate is set such that the transient response from near-surface materials will decay to very small values, and the transient response from shallow-buried (< 2 to 3 m) metallic objects will dominate the superimposed measurement result (Butler et al 1998b). However, spatial variability in the conductivity will result in a small background noise component that will increase as the conductivity and its variability increase. Since the conductivity of metallic ordnance is of the order  $10^7$  S/m, only when the object is small and/or buried at depths > 2 to 3 m will the background geologic noise become a serious impediment to ordnance detection by TDEM (Barrow, Khadr, and Nelson 1996). The metallic ordnance to surrounding material conductivity contrast is typically  $10^9$  at JPG. The magnetic susceptibility variation over the 40-acre site poses a similar though potentially greater implication for UXO detection with TDEM methods than does conductivity (Das et al. 1990). The ferrous metallic ordnance to surrounding material *contrast* in relative magnetic susceptibility at JPG is as small as  $10^5$ .

Even though the magnetic susceptibility contrast between ordnance and geologic materials at JPG is still quite large, detection of ordnance objects can become problematic when “large volume” geologic magnetic susceptibility contrasts exist. The spatial distribution of magnetic susceptibility exhibited in Figures 12 and 13 is quite complex. It is possible, however, to qualitatively examine the magnetic field anomaly along a profile. A two-dimensional total field magnetic anomaly calculation is performed for line K (Figure 13). For the calculation, rectangular cross-section cylinders are used with approximate widths and magnetic susceptibility values from Figure 13, an assumed thickness of 1 m, and infinite length perpendicular to the profile. Results of the calculation, using a program based on the familiar line integral method (Talwani and Heirtzler 1964; Thorarinsson 1985), are shown in Figure 15. The maximum positive and negative values from the calculation are consistent with the measured values discussed previously. The abrupt changes in susceptibility in the model are responsible for the spiked appearance of the calculated anomaly. Including many more cylinders in the susceptibility model to simulate the transitional changes in susceptibility, would smooth the calculated anomaly. The complexity of the calculated anomaly and the horizontal

gradients are consistent with the measured magnetic anomaly. Detection of ordnance with comparable or smaller magnetic signatures is problematic in this setting.

The most significant implications of geophysical parameters and their spatial and time variability for ordnance detection at JPG are for GPR. The conductivity maps in Figure 6, frequently good predictors of GPR “performance,” suggest variable GPR performance over the 40-acre site at a given time. A widely quoted criteria for qualitative prediction of GPR “performance” is based on conductivity: < 10 mS/m — excellent; 10 to 30 mS/m — marginal to good; > 30 mS/m — poor or problematic. The dry conditions map indicates conductivities ranging from 10 mS/m to > 30 mS/m. The data in Figure 6 and Table 4 suggest variable GPR performance as a function of environmental site conditions. For *dry conditions*, GPR performance in terms of depth of investigation should be fair to good for UXO detection nearly everywhere on the 40-acre site.

Two guidelines used for estimating depth of investigation  $d_{max}$  for GPR are (Annan and Cosway 1992; Annan and Chua 1992):  $d_{max} < 30 / \alpha$  and  $d_{max} < 35 / \sigma$ , where  $\sigma$  is the EM attenuation in dB/m,  $\sigma$  is the conductivity in mS/m, and  $d_{max}$  is in m. These guidelines are based on experience with GPR in a variety of geologic settings and transmitter frequencies and the fact that most commercial GPR’s “can typically afford to have a maximum of 60 dB attenuation associated with conduction losses (Annan 1997).” For the maximum in the attenuation and conductivity ranges for dry site conditions in Table 4,  $d_{max}$  is 3.5 m for both rules-of-thumb. Depth predictions using the dry site condition conductivities from Figure 6 range from ~1 to 3.5 m. UXO detection with GPR for *dry site conditions* at JPG should be possible to depths of ~3 m in many areas. For the extreme wet site conditions (Table 4), the guidelines give estimates of depth of investigation ranging from 0.5 to 2 m, with  $d_{max} < 1$  m, most likely. Since the Table 4 properties are for depths < 1 m, GPR detection of UXO greater than 1-m depth will be problematic for wet site conditions.

GPR considerations thus far do not specifically address the issue of frequency dependence of depth of investigation. GPR surveys conducted at JPG as part of the supplemental site characterization work (Arcone et al 1998; Llopis et al 1998) utilized different center frequency antennae. The references document the first reliably reported detection of UXO at JPG by GPR. The following tabulation lists depth of penetration achieved as a function of frequency for intermediate or moist site conditions.

<b>Center Frequency, MHz</b>	<b>Depth, m</b>	<b>Type Target</b>	<b>Comments</b>
50	> 3.5 m	Geologic Interface	Depth of detection for localized high-contrast feature likely greater
100	> 2 m	Geologic Interface	See Above
200	> 1 m	Interface; Localized Feature	See Above
300	1 m 2–3 m	UXO Noise/Attenuation Limit	Well-defined UXO signatures; Arcone et al (1998)
600	< 0.5 m < 1 m	UXO Noise/Attenuation Limit	High Attenuation at this Frequency

Another important factor in terms of detection implications is the antenna beamwidth in the subsurface, which depends on dielectric permittivity. For example, the mean value of the real part of the relative dielectric permittivity, determined from an analysis of 118 GPR diffraction signatures acquired at JPG, is 10.4. For this permittivity value and commercial dipole antennas, the beamwidth perpendicular to the profile direction (in the plane of antenna polarization) is 22 degrees (Llopis et al 1998; Arcone et al 1998). This implies that a UXO would need to lie in or very close to the plane of the profile to insure detection, since out of plane reflections/diffractions will be highly attenuated. For the considerably higher permittivity values for some areas of the site, particularly for wet site conditions, the beamwidth becomes even smaller.

## Conclusions

Implications of wet versus dry site conditions for GPR detection of buried ordnance at JPG are significant. Ordnance buried below the near-surface high water content zone, during wet site conditions, may *not* be detectable, while the same ordnance may be detectable during dry site conditions. Likewise for the TDEM method, the high water content near surface zone will have increased soil conductivity, resulting in a decreased conductivity contrast and a decreased signal to noise ratio. While the actual ordnance detection implications for TDEM are minor, cases where ordnance detection are predicted to be marginal under dry conditions, may be *undetectable* under wet site conditions. At locations where the clay layer is shallow and ordnance items are buried within the layer, detection by GPR becomes problematic for any site condition. Also, the electrical conductivity contrast is reduced for ordnance items buried in the clay layer, decreasing the signal to noise ratio for TDEM surveys. Above the clay layer, the material is predominantly very fine-grained quartz, with only small amounts of clay minerals. High dielectric permittivity values at the site results in small GPR antennae beamwidths perpendicular to the survey line direction.

There is a significant spatial variation in near-surface magnetic susceptibility. The magnetic susceptibility of materials in the upper 0.5 m of the site can vary by an order of magnitude over horizontal distances of 2 to 3 m. The magnetic susceptibility variations produce magnetic anomalies that significantly interfere with detection of the magnetic anomalies of buried ordnance and also can reduce the magnetic susceptibility contrast, decreasing the signal to noise ratio for magnetic surveys. The most significant of these magnetic anomalies generally correlate spatially with the major drainage features of the site.

Examination of high-resolution, high-accuracy total magnetic field anomaly maps of the 40-acre site, reveals that the magnetic background (noise levels) areas of the 40-acre site vary from “quiet” ( $< \pm 5$  nT) to noisy ( $\sim \pm 20$  nT). The predicted total magnetic field anomalies for the Phase II and III baseline ordnance items indicates the minimum peak positive anomaly magnitude for Phase III is 18 nT, while some Phase II baseline ordnance targets have anomaly values  $< 10$  nT (Butler et al 1999). For the magnetically quiet areas of the site, only some of the Phase II baseline ordnance targets are difficult to detect. For magnetically noisy areas of the site, however, a small number of Phase III ordnance targets and a significant number of Phase II targets become difficult to detect.

EM61 TDEM maps indicate considerable areas with background noise levels  $< \pm 2$  mV, although some areas have noise levels  $\sim \pm 5$ – $10$  mV. While only a small number of Phase III ordnance targets are difficult to detect with an EM61-type TDEM system, a significantly larger number of Phase II targets could be difficult to detect, depending on the burial location at the site (Butler et al 1999).

The results documented here indicate the need to evaluate the results of UXO detection surveys based on site-specific criteria. That is, the probability of detection and false alarm rates can vary considerably over a survey area based on site specific geologic and soil conditions. Selection of appropriate geophysical survey methods should be guided by a priori assessment of geology, soil, and geophysical parameter variations. Geophysical signature modeling of expected ordnance types and depths should be conducted, with site-specific signal to noise considerations, to guide survey planning. Likewise, assessment of the results of geophysical surveys for UXO detection should be performed with cognizance of the site-specific conditions.

## Acknowledgment

The authors appreciate the assistance of Drs. Nagi Khadr and Bruce Barrow, AETC, Inc., and Drs. Herbert Nelson and James McDonald, Naval Research Laboratory (NRL), in this work. NRL provided JPG geophysical survey data, and AETC assisted with specialized presentations of the data.

## References

- Altshuler, Thomas W., Andrews, Anne M., Dugan, Regina E., George, Vivian, Mulqueen, Michael P., and Sparrow, David A. (1995). “Demonstrator performance at the unexploded ordnance advanced technology demonstration at Jefferson Proving Ground (Phase I) and implications for UXO clearance,” IDA Paper F-3114, Institute for Defense Analyses, Alexandria, VA.
- Annan, A. P. (1997). *Ground penetrating radar workshop notes*. Sensors and Software, Inc., Mississauga, Ontario, Canada.
- Annan, A. P. and Cosway, S. W. (1992). “Ground penetrating radar survey design,” *Proceedings of the Symposium on Application of Geophysics to Engineering and Environmental Problems, SAGEEP 92*, Oakbrook, IL, 329-351.

- Annan, A. P. and Chua, L. T. (1992). "Ground penetrating radar performance predictions," Paper 90-4, The Geological Survey of Canada, 5-13.
- Arcone, Steven A., Delaney, Allan J., Sellmann, Paul V., and O'Neill, Kevin. (1998). "UXO detection at Jefferson Proving Ground using ground-penetrating radar," *Proceedings of the UXO Forum 1998* (24 p, CD ROM).
- Barrow, Bruce, Khadr, Nagi, and Nelson, Herbert H. (1996). "Performance of electromagnetic induction sensors for detecting and characterizing UXO," *Proceedings of the UXO Forum 1996*, Williamsburg, VA, 308-314.
- Bartington Instruments LTD. (1994). *Operation manual for MS2 Magnetic Susceptibility System*. OM0408 Issue 1, Bartington Instruments LTD, Oxford, UK.
- Burger, H. Robert. (1992). *Exploration geophysics of the shallow subsurface*. Prentice Hall, Englewood Cliffs, NJ.
- Butler, Dwain K. (1975). "An analytical study of projectile penetration into rock," Technical Report S-75-7, U.S. Army Engineer Waterways Experiment Station, Vicksburg, MS.
- Butler, Dwain, Cespedes, Ernesto, O'Neill, Kevin, Arcone, Steven, Llopis, Jose, Curtis, John, Cullinane, John, Meyer, Clemens. (1998). "Overview of Science and Technology Program for JPG Phase IV," *Proceedings of the UXO Forum 98*, Anaheim, CA (10 p, CD ROM).
- Butler, Dwain K., Llopis, Jose L., and Simms, Janet E. (1999). "Phenomenological investigations of the Jefferson Proving Ground UXO technology demonstrations," Technical Report GL-99-\_, U.S. Army Engineer Research and Development Center, Vicksburg, MS.
- Cassagrande, A. (1948). "Classification and identification of soils." *Transactions of the American Society of Civil Engineers*, 113.
- Das, Yogadhis, McFee, John E., Toews, Jack, Stuart, Gregory C. (1990). "Analysis of an electromagnetic induction detector for real-time location of buried objects," *IEEE Transactions on Geoscience and Remote Sensing*, 28 (3), 278-288.
- Dearing, John. (1994). *Environmental magnetic susceptibility using the Bartington MS2 System*. Chi Publishing, Kenilworth, UK.
- Isaaks Edward H., and Srivastava, R. Mohan. (1989). *An introduction to applied geostatistics*. Oxford University Press, New York.
- Keller, George V., and Frischknecht, Frank C. (1970). *Electrical methods in geophysical prospecting*. Pergamon Press, New York.
- Khadr, Nagi, Bell, Thomas, Williams, Scott, Bacon, William B. (1997). "UXO detection in highly magnetic soils," *Proceedings of the UXO Forum 97*, 222-228.
- Llopis, Jose L., Simms, Janet E., Butler, Dwain K., Curtis, John O., West, Harold W., Arcone, Steven A., and Yankielun, Norbert E. (1998). "Site characterization investigations in support of UXO technology demonstrations, Jefferson Proving Ground, Indiana," Technical report GL-98-20, U.S. Army Engineer Waterways Experiment Station, Vicksburg, MS.
- McDonald, James R. and Nelson, Herbert H. (1999). "Results of the MTADS technology demonstration #3," NRL/PU/6110-99-375, Naval Research Laboratory, Washington, DC.
- McNeill, J. D. (1986). "Geonics EM38 ground conductivity meter, Operating instructions and survey interpretation techniques," Technical Note TN-21, Geonics Limited, Mississauga, Ontario, Canada.
- McWilliams, Kendall M. (1985). *Soil survey of Ripley County and part of Jennings County, Indiana*. Soil Conservation Service, U.S. Department of Agriculture, Washington, DC.
- Means, R. E. and Parcher, J. V. (1963). *Physical properties of soils*. Charles E. Merrill Publishing Co., Columbus, OH.
- Miller, C. A., Malone, C. R., and Blount, C. B. (1992). "Guide for the conduct of predeployment site characterization surveys for the AN/GSS-34 (V) Ported Coaxial Cable Sensor (PCCS)," Instruction Report EL-92-1, U.S. Army Engineer Waterways Experiment Station, Vicksburg, MS.
- Nickell, Allan K. (1985). *Soil survey of Jefferson County, Indiana*. Soil Conservation Service, United States Department of Agriculture, Washington, DC.
- PRC Environmental management, Inc. (1994). "Geotechnical investigation report," Task 3: Preparation of demonstration site, Jefferson Proving Ground, Indiana, U.S. Naval Explosive Ordnance Disposal Technology division, Indian head, MD.
- Sahimi, Muhammad. (1995). *Flow and transport in porous media and fractured rock*. VCH Verlagsgesellschaft mbH, Weinheim, FRG.
- Scollar, I., Tabbagh, A., Hesse, A., Herzog, I. (1990). *Archaeological prospecting and remote sensing*. Cambridge University Press, New York.
- Talwani, M., and Heirtzler, J. R. (1964). "Computation of magnetic anomalies caused by two-dimensional structures of arbitrary shape," *Computers in the Mineral Industry, Part 1*, Stanford University Publications, 464-480.

- Thorarinsson, Freyr. (1985). "Two-dimensional graphically interactive modeling of gravitational and magnetic anomalies," Digitus International, Golden, CO.
- USAEC. (1995). "Evaluation of individual demonstrator performance at the unexploded ordnance advanced technology demonstration program at Jefferson Proving Ground (Phase I)," Report No. SFIM-AEC-ET-CR-95033, U.S. Army Environmental Center, Aberdeen Proving Ground, MD.
- USAEC. (1996). "Unexploded ordnance advanced technology demonstration program at Jefferson Proving Ground (Phase II)," Report No., SFIM-AEC-ET-CR-96170, U.S. Army Environmental Center, Aberdeen Proving Ground, MD.
- USAEC. (1997). "UXO Technology Demonstration Program at Jefferson Proving Ground, Phase III," Report No. SFIM-AEC-ET-CR-97011, U.S. Army Environmental Center, Aberdeen Proving Ground, MD.

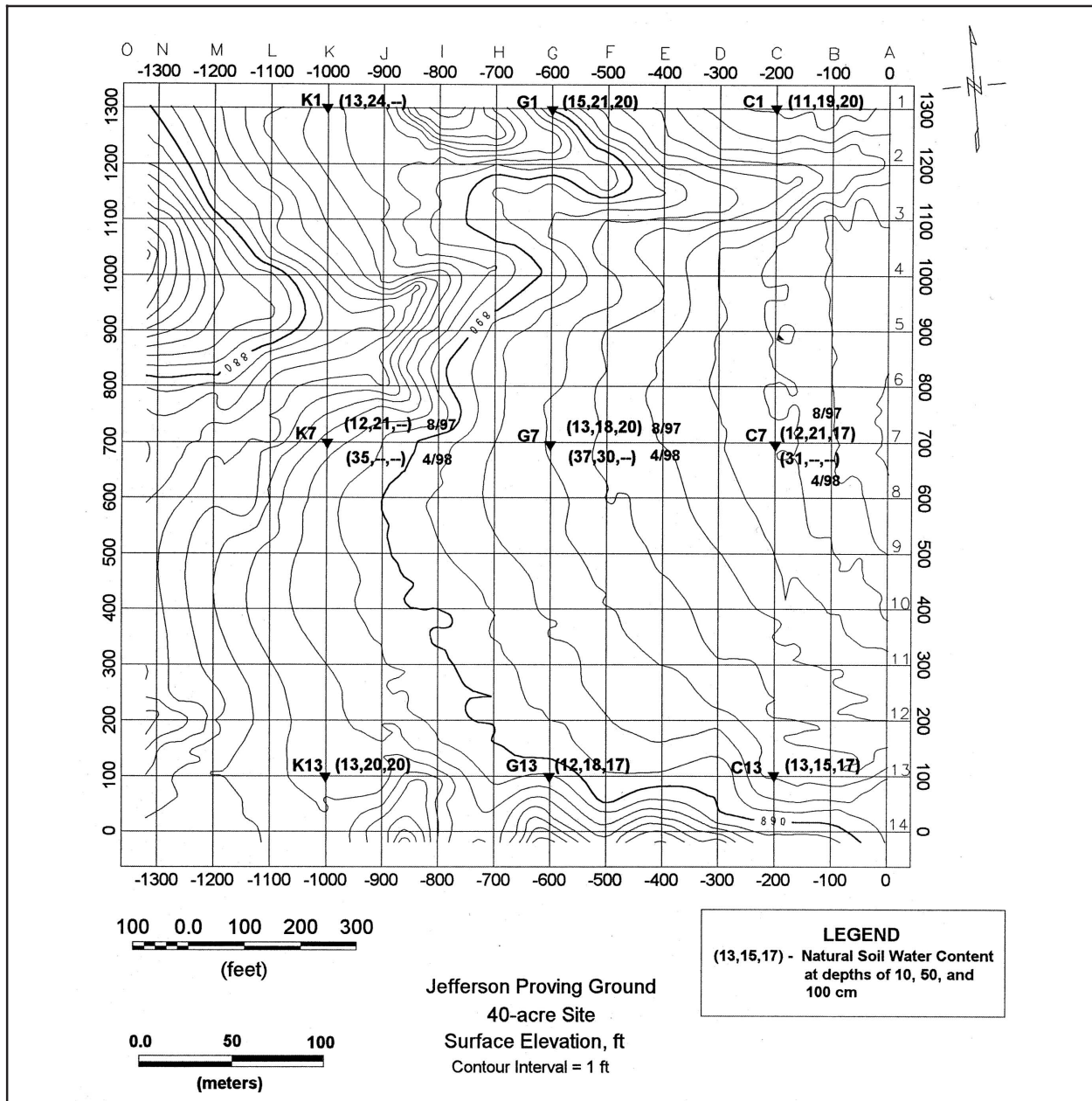


Figure 1. JPG 40-acre site map, showing nine locations where water contents were determined for 10-, 50-, and 100-cm depths for dry site conditions (8/97) and three sites where water contents were determined for wet site conditions (4/98)

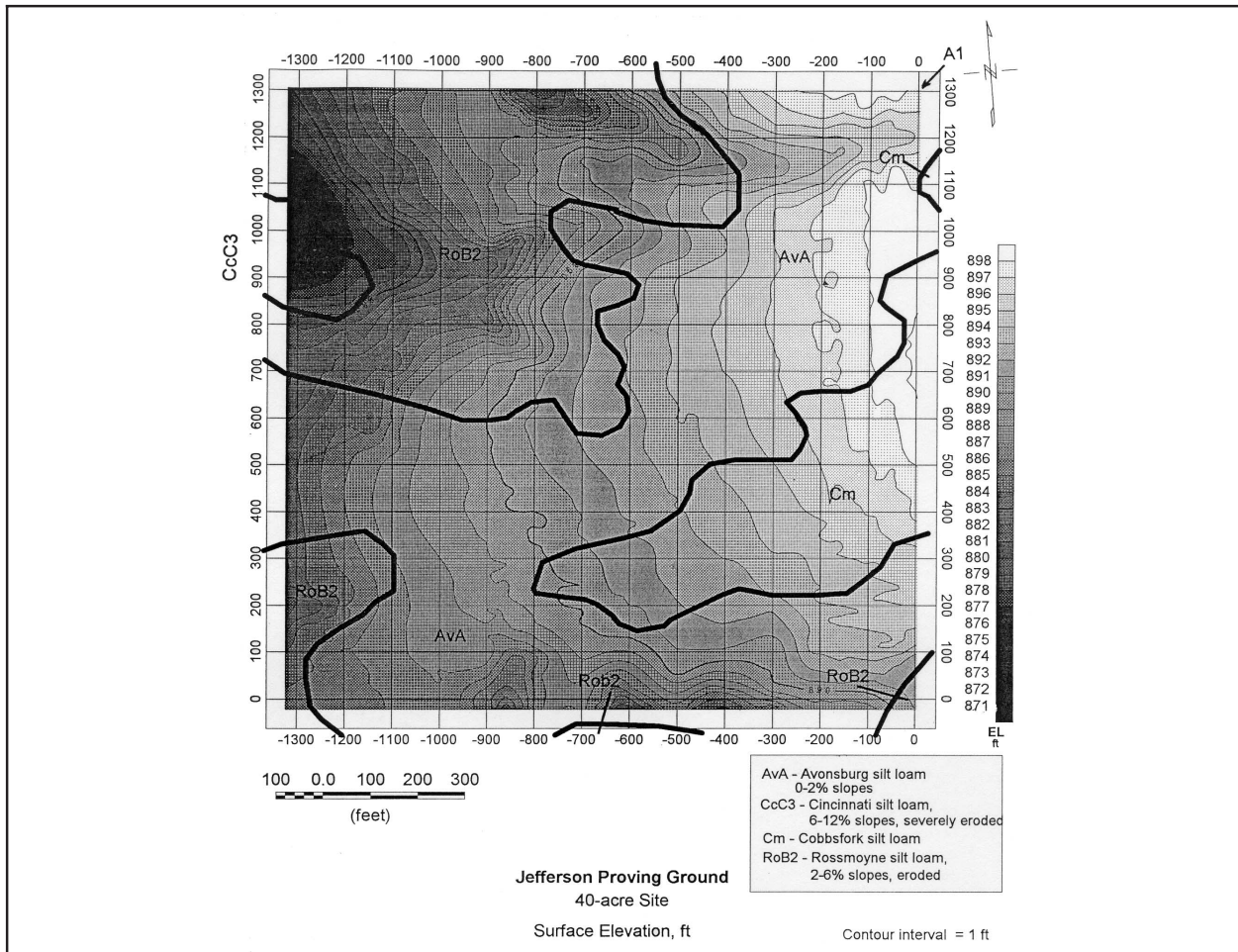


Figure 2. JPG 40-acre site: soils map superimposed on topography

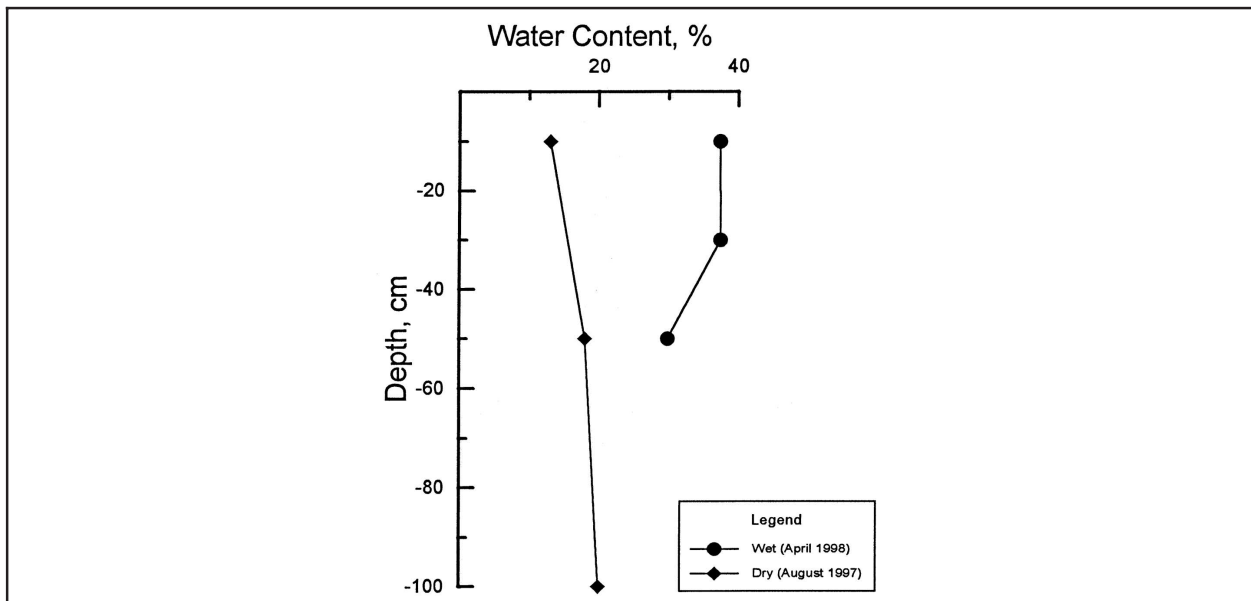


Figure 3. Variation of soil water content with depth for wet and dry site conditions at location G7, 40-acre site

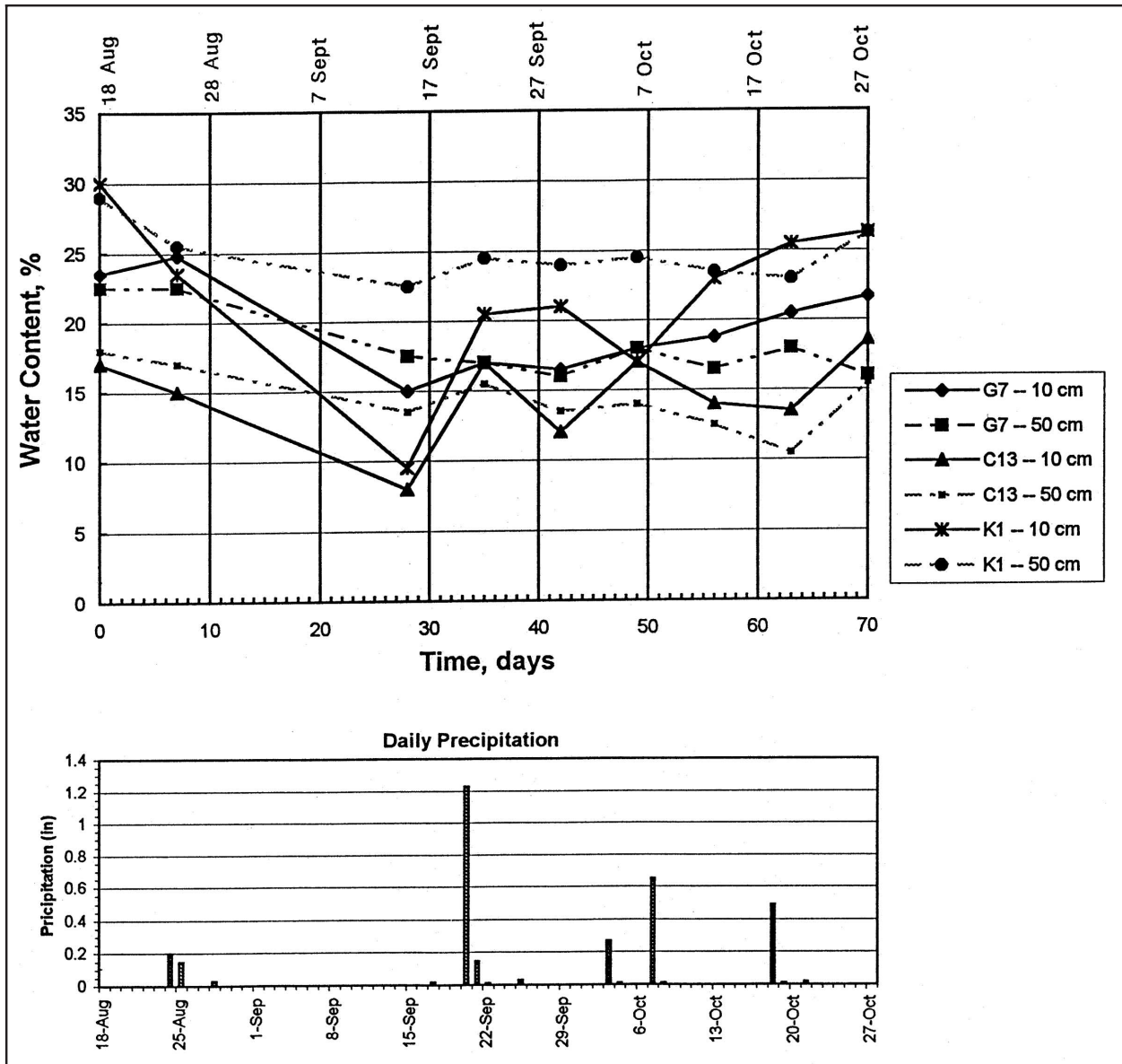


Figure 4. Natural water contents, for two depths and three locations, and precipitation during JPG Phase IV demonstrations



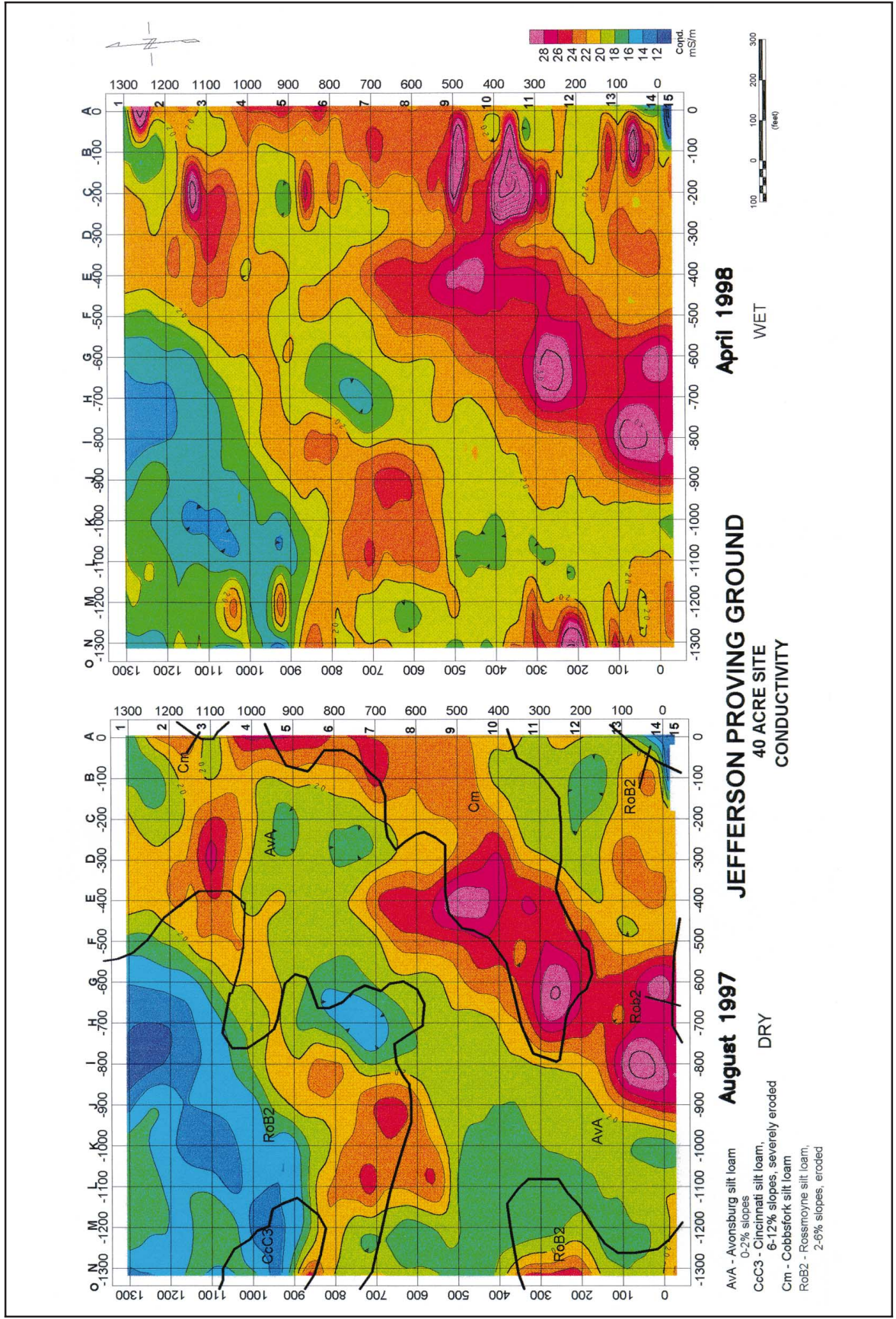


Figure 6. Electromagnetic terrain conductivity map for 40-acre site during dry (left) and wet (right) site conditions; determined with Geonics EM-31 (frequency domain EM induction system, 9.8 kHz)

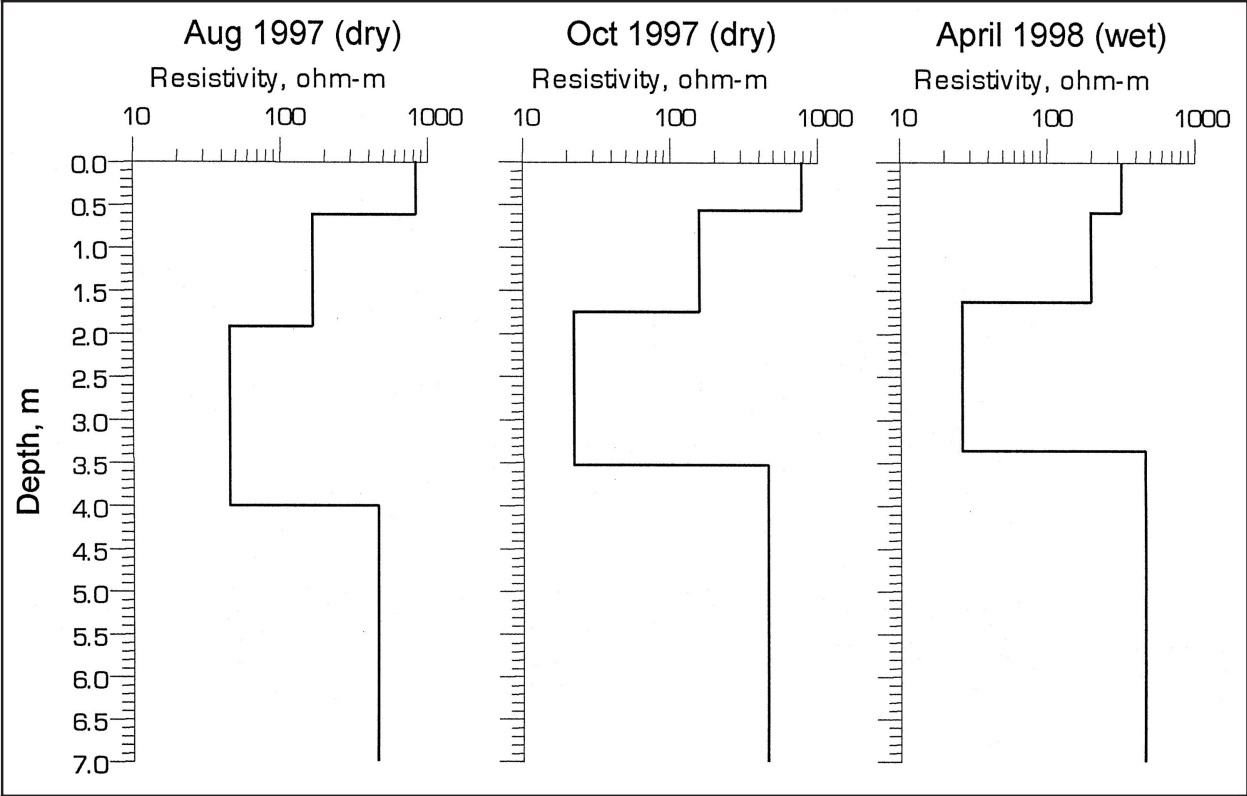


Figure 7. Electrical resistivity sounding interpretations for three dates at Location G7, 40-acre site

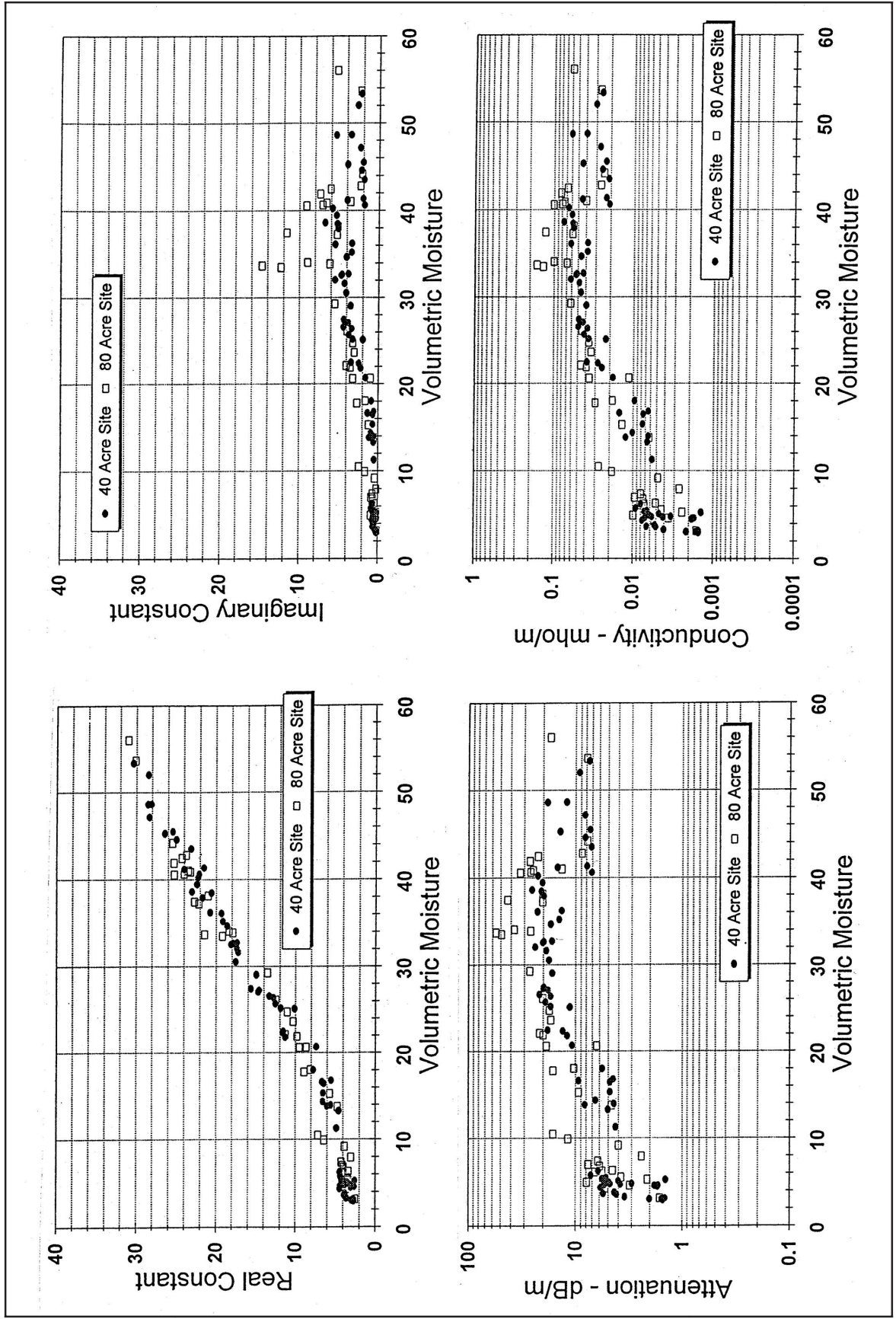


Figure 8. Example of laboratory electromagnetic properties measurements for shallow JPG soils at 200 MHz as a function of volumetric moisture content (Llopis et al 1998)

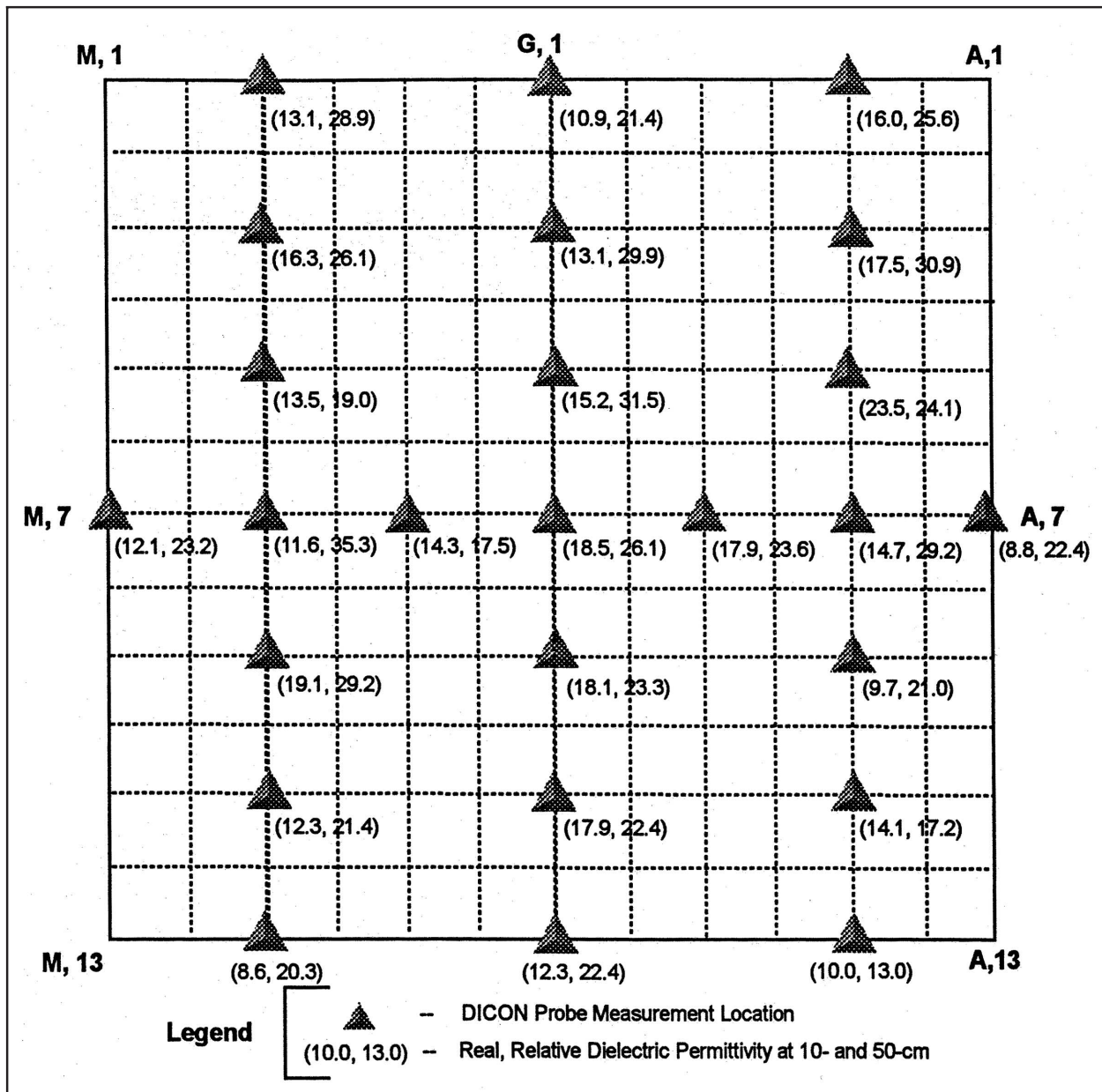


Figure 9. DICON probe measurements of the real component of the complex dielectric permittivity at 10- and 50-cm depths at the 40-acre site

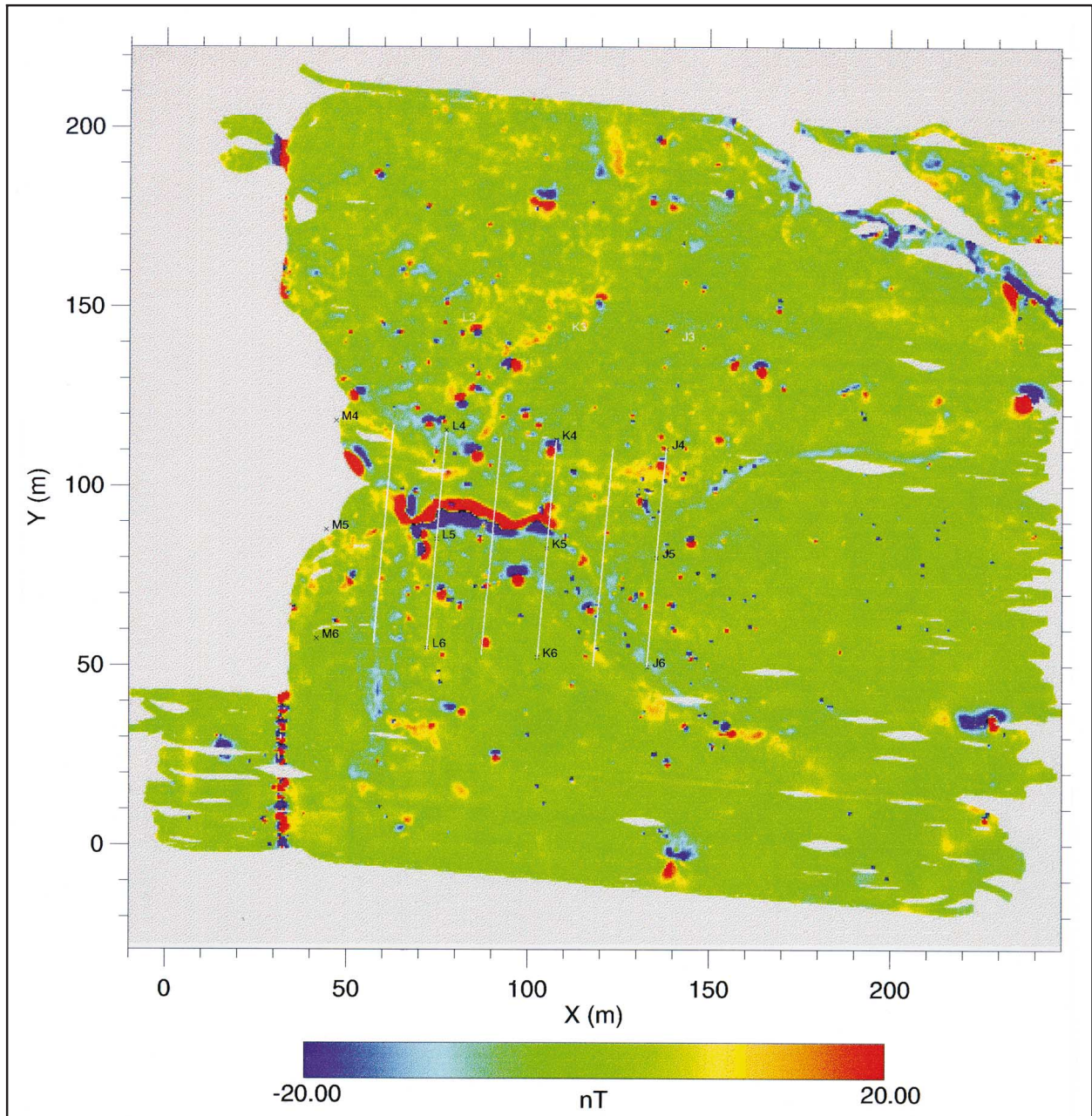


Figure 10. Phase III Naval Research laboratory MTADS total magnetic field map of northwest quadrant of 40-acre site

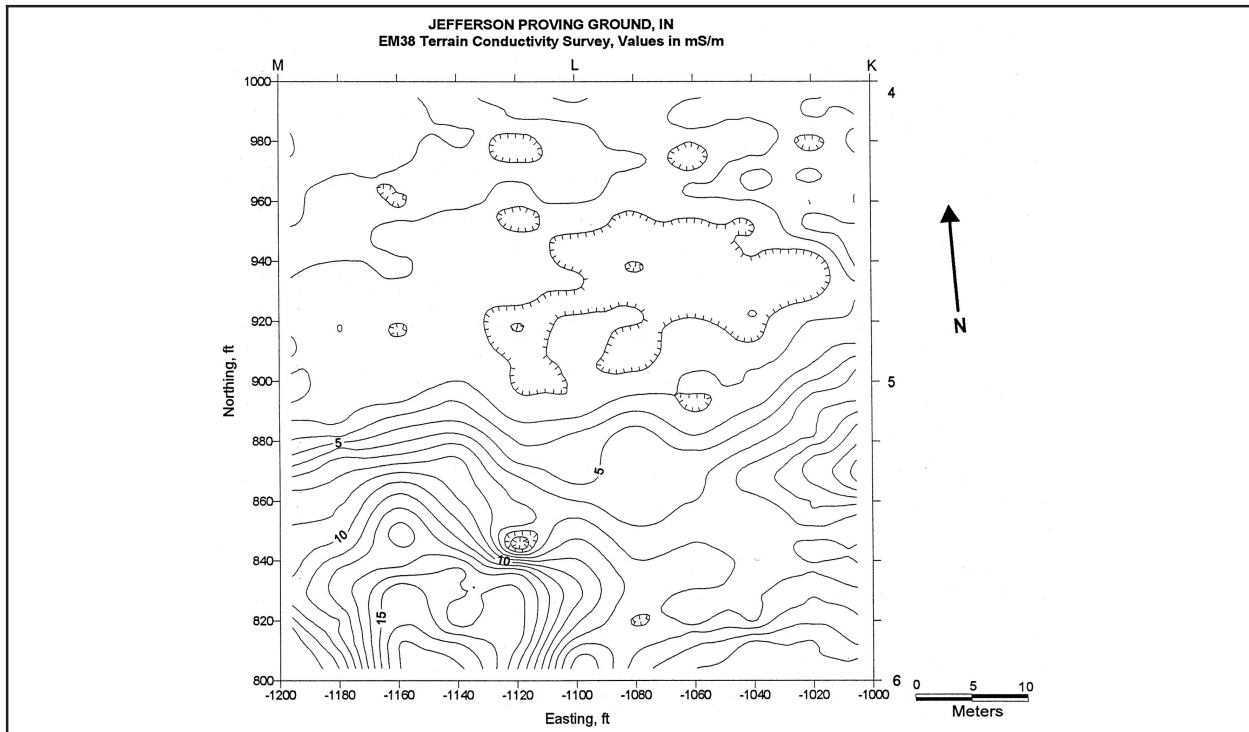


Figure 11. Terrain conductivity map determined with Geonics EM-38 (frequency domain EM induction system, 14.6 kHz) of a portion of the northwest quadrant of the 40-acre site, approximately centered on the anomalous magnetic feature shown in Figure 10

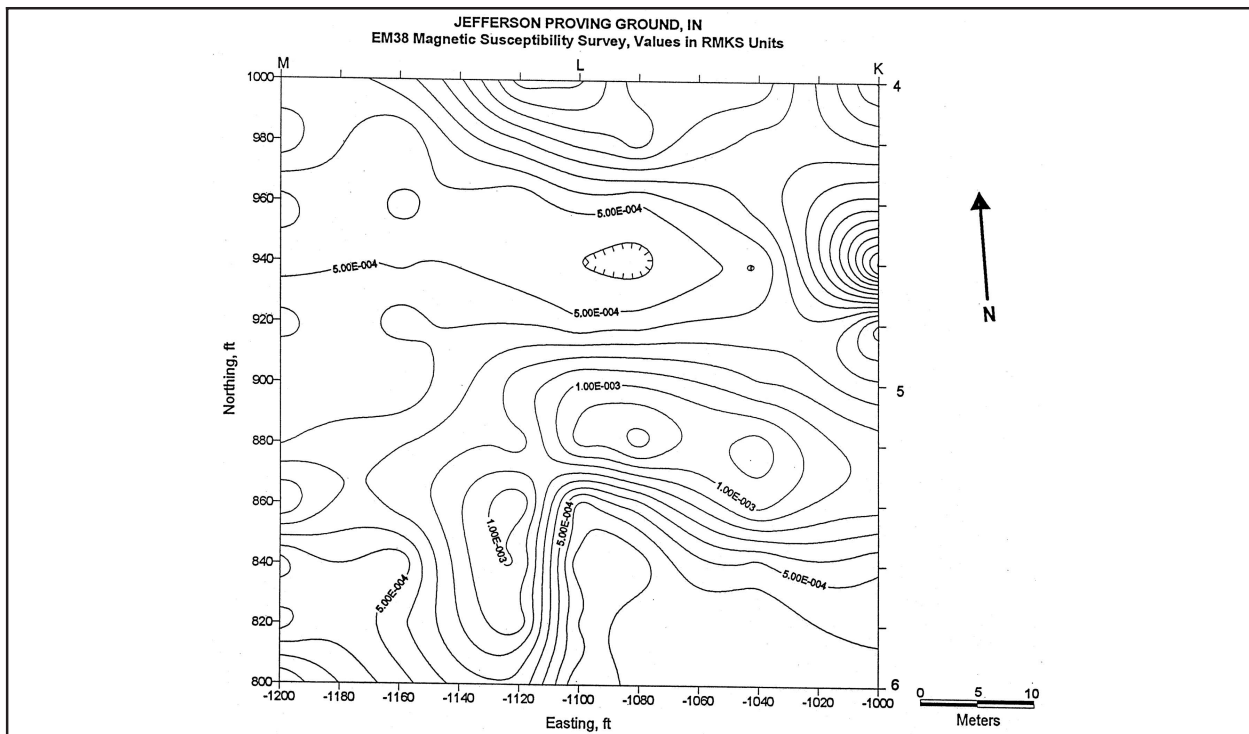


Figure 12. Magnetic susceptibility map (SI units) of a portion of the northwest quadrant of the 40-acre site, corresponding to the area shown in Figure 11 and approximately centered on the anomalous magnetic feature shown in Figure 10

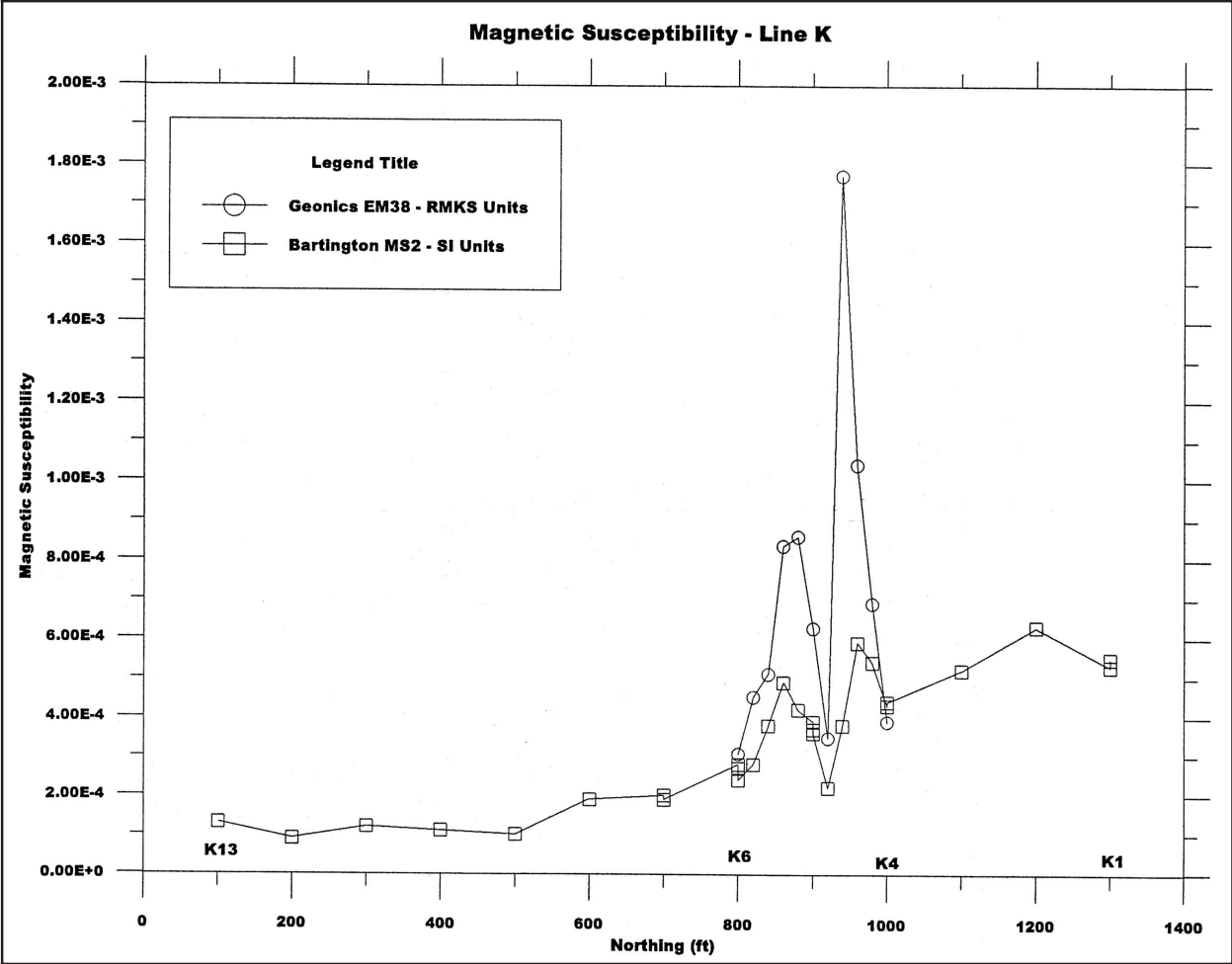


Figure 13. Magnetic susceptibility profiles along grid line K, from K13 to K1

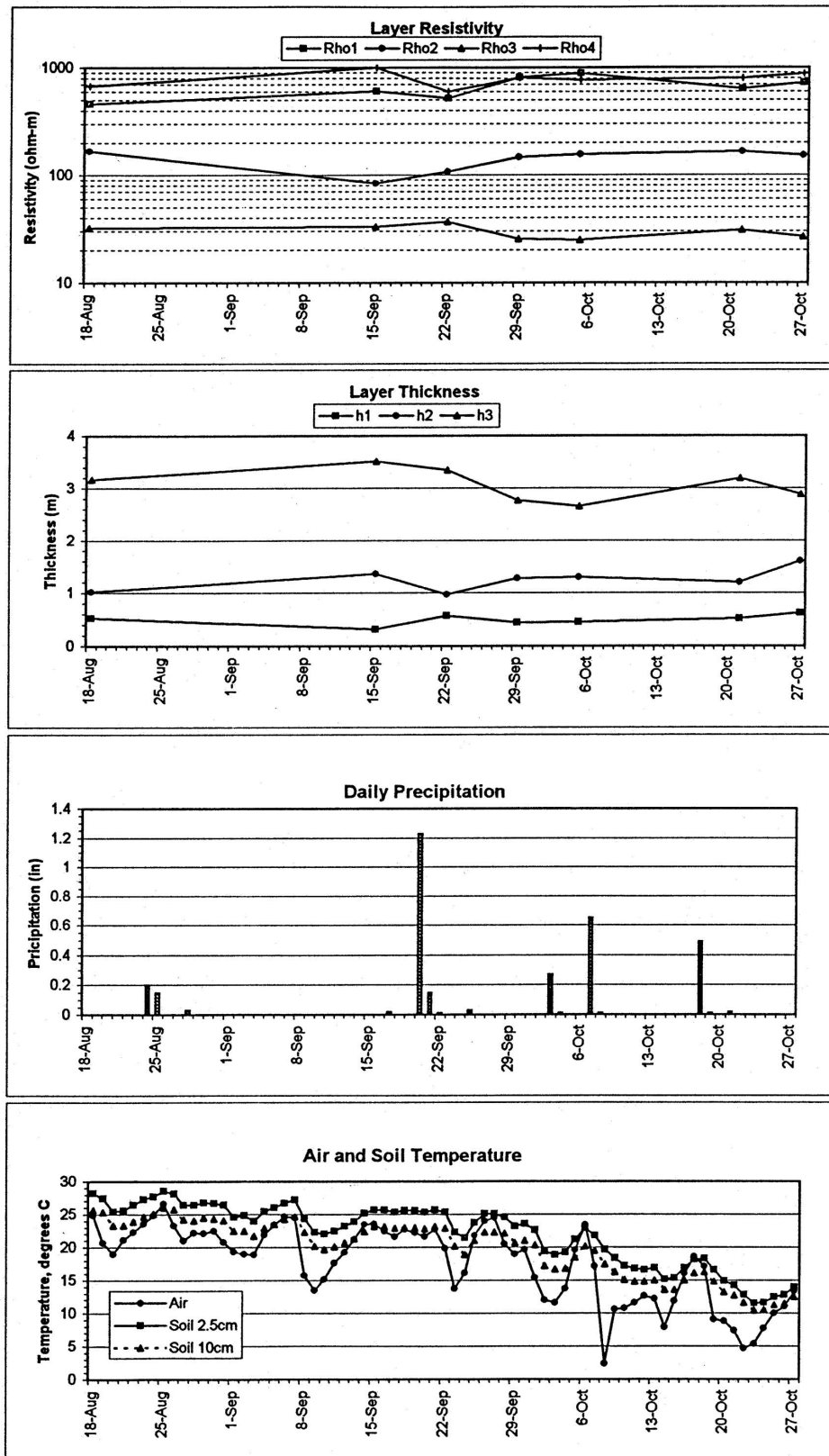


Figure 14. Electrical resistivity model parameters, precipitation, and air and soil temperatures as a function of date during the Phase IV demonstrations

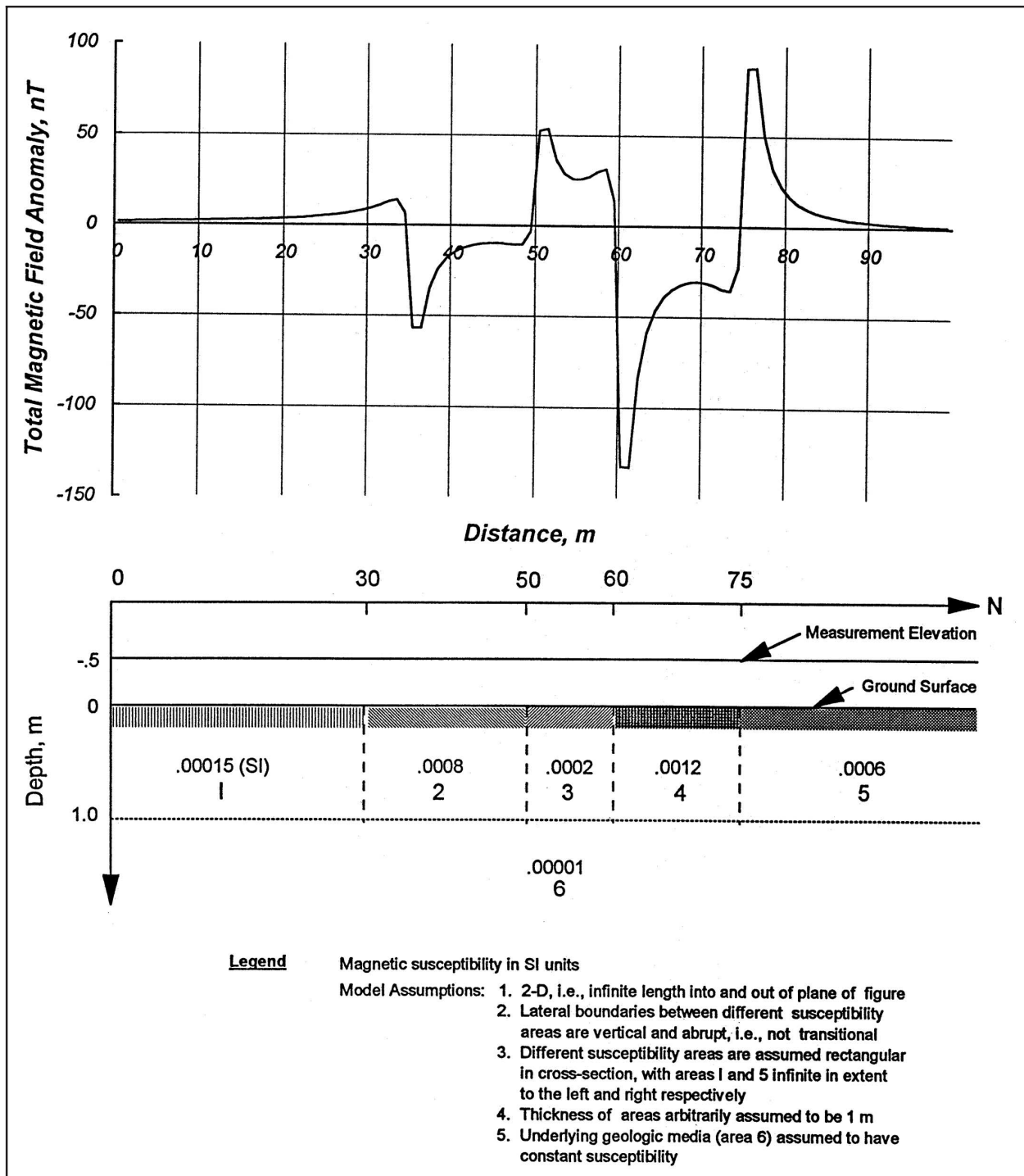


Figure 15. Total magnetic field anomaly calculations (2-D) for hypothetical model of susceptibility along line K based on susceptibility measurements (Figure 13)